Surg Radiol Anat (2010) 32:115–122
DOI 10.1007/s00276-009-0563-2

ORIGINAL ARTICLE

Internal architecture of calcaneus: correlations with mechanics and pathoanatomy of calcaneal fractures

Sunita Arvind Athavale · Subhash D. Joshi · Sharda S. Joshi

Received: 11 January 2009 / Accepted: 7 September 2009 / Published online: 24 September 2009

Abstract
Background Available studies on internal architecture of the calcaneus are cursory and contradictory. Present study focused on elaborate descriptions of the different trabecular groups and their correlation with the fractures of this bone.
Method To study the internal architecture, 50 dry adult human calcanei were sectioned in various planes and grossly dissected.
Results Six different groups (A–F) of lamellae were identified. Based on the observations of trabecular architecture, potential weak areas in this bone were identified. The predicted weak zones correlate well with the fracture lines described in the calcaneus and provide anatomical basis for their occurrence.
Conclusions This study underscores the major influence of the internal architecture of the calcaneus in predicting the fracture lines. The findings can be utilized to classify fractures of calcaneus, which has been a topic of ongoing debate. Knowledge of weak zones will aid clinicians to improve the techniques of internal fixation.

Keywords Calcaneus · Compressive forces · Fracture lines · Lamellae · Tensile forces · Trabecular architecture

S. A. Athavale (✉)
Department of Anatomy, KVG Medical College, Sullia, D.K. District 574327, Karnataka, India
e-mail: arvindat@rediffmail.com

S. D. Joshi · S. S. Joshi
Department of Anatomy, Rural Medical College, PIMS Loni, Ahmednagar, Maharashtra, India

Introduction

The calcaneus is the largest of the tarsal bones which provides an elastic but firm support for the weight of the body. It forms a more vertical, shorter and less yielding posterior limb of the longitudinal arches of foot. The functions served by calcaneus during normal gait are (1) to act as lever arm powered by gastrocnemius and soleus muscles, (2) to provide a foundation for support for the body weight and (3) to provide support and maintain the length of the posterior column of the foot. Approximately 50% of the weight bearing of the foot occurs through the calcaneus [5].

Given the pre-eminent mechanical function of the calcaneus, attempts at demonstrating the trabecular trajectories and their correlation with mechanical role of calcaneus date back to eighteenth and early nineteenth centuries [28, 30, 32]. More recently, radiographic, anatomical and neutron diffraction studies have dealt with the internal architecture of this bone [3, 24, 26, 29]. Few biomechanical studies have dealt with mechanical adaptation of calcaneus [11, 15].

Calcaneus is the most frequently fractured bone among all the tarsal bones. Classification of the fractures of the calcaneus has been a matter of intense investigation [4, 21, 25, 36]. The highly variable fracture pattern is attributed to the magnitude and direction of the impacting force, the foot position, the muscular tone, and the mineral content of the bone [8, 18, 23]. Some experimental studies have been conducted on the mechanism of causation of fracture lines in the calcaneus [5, 6, 22, 34, 35]. These studies have focused on effect of type and amount of force causing primary and secondary fracture lines and the description of those lines and fragments of the calcaneus.

The development of fracture lines in any bone is a result of multiple factors. Structure of the bone (both external and

internal) is also an important determinant of formation of fracture lines. However, correlation of internal architecture and its role in predicting fracture lines has remained an inadequately explored area so far.

Although illustrations of the calcaneal trabecular pattern have been often repeated, review of literature, however, highlights that comprehensive and original descriptions of internal architecture of calcaneus are few, cursory and contradictory. Also, the available descriptions do not provide elaborate accounts of different groups of lamellae. So, the objective of this study was to perform a detailed study of internal architecture of the calcaneus and correlate it with the fractures of this bone.

Materials and methods

Fifty (25 right; 25 left) dry adult calcanei were used for the present study. Sex of these bones was not known. Bones were apparently normal and free of any congenital malformation. To study the trabecular pattern, the bones were sectioned into slices of 3–4 mm thickness with the help of a band saw. Twelve bones each (6 right; 6 left) were cut in sagittal and coronal planes, while 10 bones (5 right; 5 left) were cut in the horizontal plane. Sixteen bones (8 rights; 8 left) were grossly dissected by removal of cortical bone with the help of a bone nibbler. To overcome the effect of loss of bone in the plane of slicing and to study the three-dimensional configuration of trabecular bone, sectioning in various planes and gross dissection of the calcaneus were planned. Grossly demineralized bones were excluded from the study. Representative sections were photographed and major lamellar patterns were sketched.

Results

Cortical shell of bone was thicker in the following areas: medial wall; inferior surface of the sustentaculum, where it became continuous with the medial wall; all articular areas (especially the post articular facet); site of attachment of tendocalcaneus; medial and lateral tubercles; area between the three plantar tubercles.

A distinct thickening of compact bone, running transversely, was seen just anterior to the lower margin of the posterior talar facet (Fig. 1a). The cortical bone along the lateral wall was thinner, especially along its antero-inferior part (Fig. 1a).

Trabecular architecture of calcaneus

Six different groups of trabeculae were observed in the calcaneus (Fig. 2a, b).

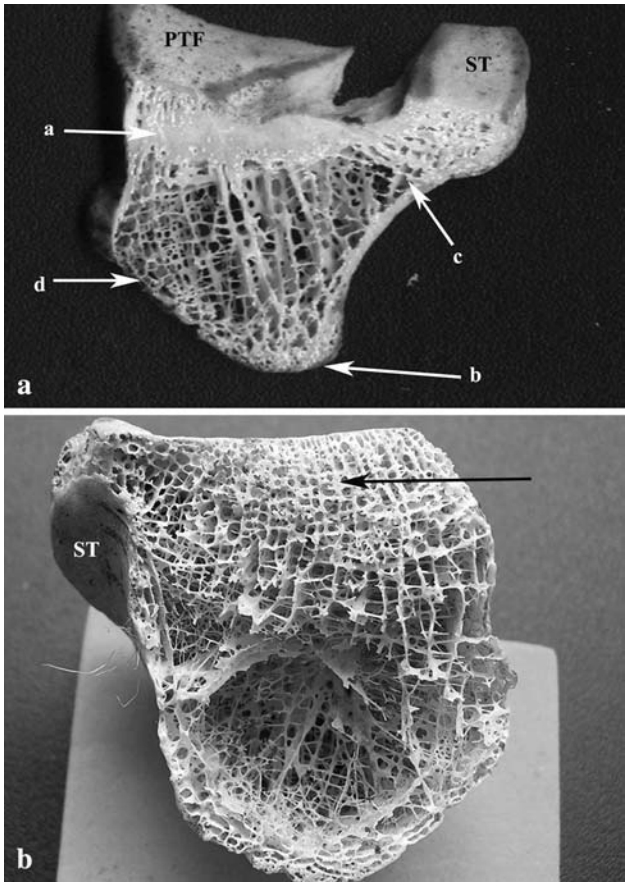

Fig. 1 **a** Coronal section of the right calcaneus, viewed from the front, showing transverse thick bony strut (*a*), present just anterior to the posterior talar facet (*PTF*); vertical lamellae descend down from this strut towards the anterior tubercle (*b*); sustentacular lamellae (Group F) are seen impinging onto the medial wall (*c*) which is thicker compared to thinner lateral wall (*d*); *ST* sustentaculum tali. **b** Coronal section of the right calcaneus, viewed from behind, showing sagittal plates deep to the posterior talar facet (*arrow*) and the horizontal cross bridges between them. *Lower part* of the specimen shows neutral zone (area of sparse trabeculae); *ST* sustentaculum tali

Group A

A distinct zone of trabeculae was seen in the form of dense closely packed parallel running bony tubes extending from the upper part of posterior talar facet to the upper one-third of the posterior surface of the calcaneus.

Group B

This group of lamellae extended from the posterior talar facet to the medial and the lateral tubercles. These were in the form of vertical interconnected bony plates, which had a sagittal orientation deep to the posterior talar facet and extended to a variable length inferiorly. The central ones had maximum height and the peripheral ones (medial and lateral) gradually decreased in height, so that in a coronal

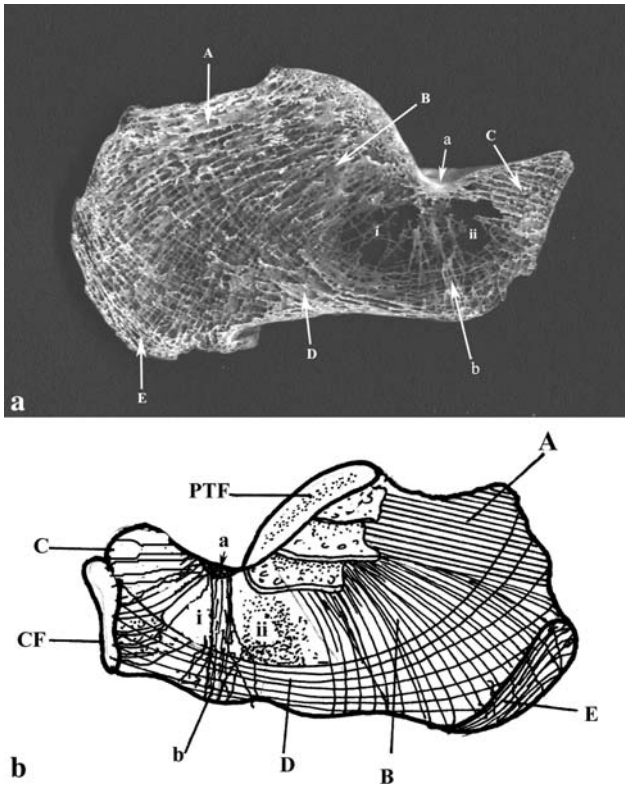

Fig. 2 **a** Sagittal section of the right calcaneus showing various groups of lamellae (*A–E*). Neutral zone is seen between Groups B and C, subdivided into two parts (*i*, *ii*) by vertical lamellae (*b*), which descend from the thick compact bone at the angle of Gissane (*a*) present in the roof of the this zone. **b** Diagram of sagittal section of calcaneus showing schematic representation of various components seen in **a**; *PTF* posterior talar facet, *CF* cuboidal facet

section their inferior ends formed a "V"-shaped area (Fig. 1b). When traced posteriorly, these plates continued as fenestrated lamellae for some distance before they broke up into thin plates which slightly diverged from one another. These plates were gradually twisted, assuming an arched course and finally led to the branching rods, which reached medial and lateral tubercles. These thick rods were interconnected by very fine meshwork of bony strands (Fig. 3).

Group C

This set continued as anterior extension from the lower edges of the sagittal plates present deep to the posterior talar facet (Fig. 4a, b). These plates impinged onto the thickened compacta, anterior to the posterior talar facet and again spread out from the same in the form of stacked bony plates. These stacked plates ran parallel to the anterior part of superior surface of calcaneus (Fig. 5a). Their lateral edges inclined down sharply and became sagittal (Fig. 5b). So, this group appeared like a pyramid with base at the cuboidal facet and apex at the thickened compacta. The orientation of

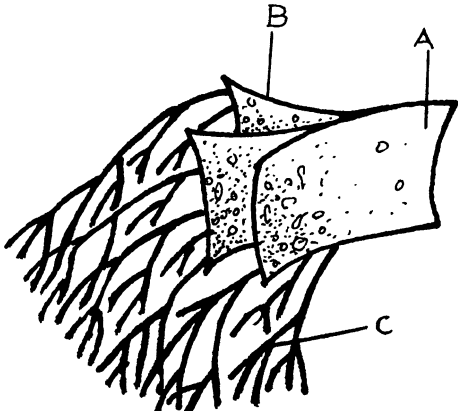

Fig. 3 Schematic diagram to show the division of sagittally oriented plates of 'Group B' lamellae. When traced posteriorly, these plates continue as fenestrated lamellae for some distance before they break up into thin secondary plates, which slightly diverged from one another. These secondary plates finally lead to the branching rods, which reach medial and lateral tubercles. *A* sagittal plate, *B* secondary plates, *C* branching rods

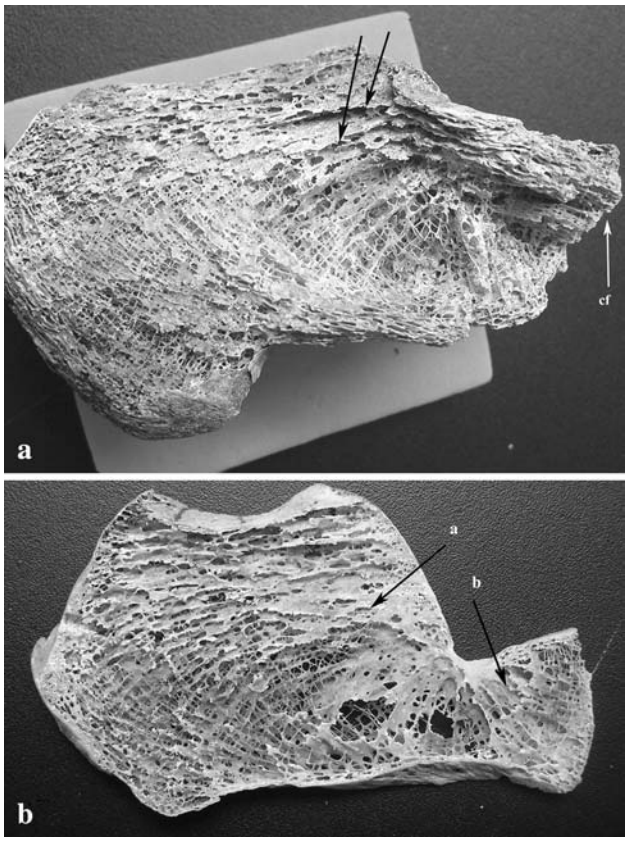

Fig. 4 **a** Gross dissection of the right calcaneus showing lower ends of sagittal plates of 'Group B' lamellae (*arrows*) continuing forwards towards cuboidal facet (*cf*). **b** Sagittal section of the left calcaneus showing sagittal plate deep to the posterior talar facet (*a*); continuity of the same plate is seen antero-inferiorly towards cuboidal facet (*b*)

these plates at the cuboidal facet (as seen in a coronal section) was like an inverted J and was similar to the orientation of cuboid bone in normal anatomical position (Fig. 6).

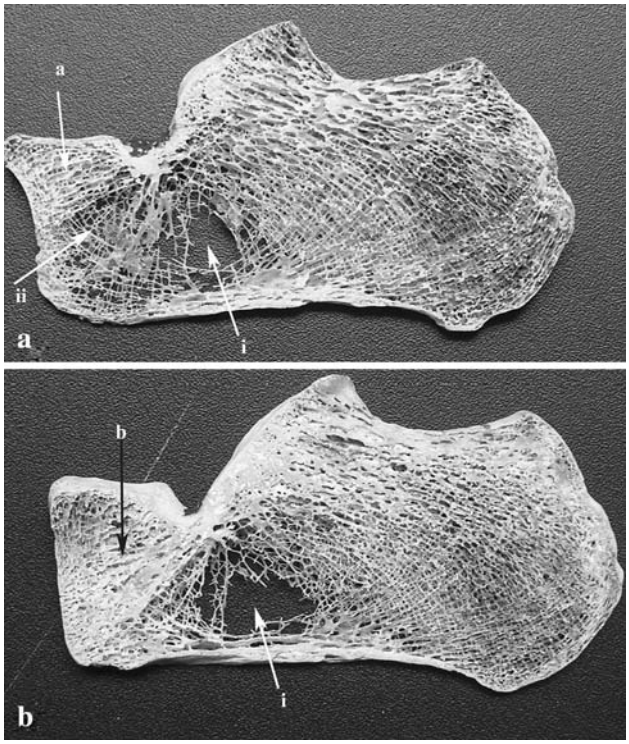

Fig. 5 Showing successive sagittal sections of the left calcaneus, viewed from lateral aspect. **a** Shows horizontal components of 'group C' lamellae (*a*); *i* and *ii* represent posterior and anterior subdivisions of neutral zone separated by a septum. **b** Shows vertical components of arched 'Group C' lamellae (*b*) which obliterate the anterior subdivision of the neutral zone

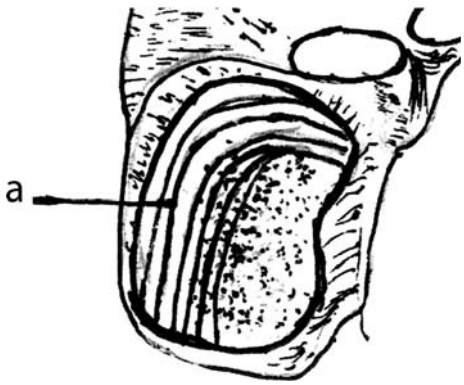

Fig. 6 Diagram of anterior surface of the calcaneus to show the arching pattern of lamellae of 'Group C' in relation to the cuboidal articular area (*a*)

Group D

These lamellae arose from the whole of the posterior surface in the form of fine rods. They extended downwards and forwards, and in this part of their course, they were seen to intersect the Group B lamellae. These lamellae converged and condensed in the form of horizontal plates, parallel to the inferior surface of the calcaneus, in the area deep to the attachment of long plantar ligament. Traced anteriorly, they again diverged in the form of rods, intersected Group C lamellae and reached up to the cuboidal articular facet (Fig. 2a, b).

Group E

Extending from the area of attachment of the tendocalcaneus, stacked plates running parallel to the lower part of posterior surface of the calcaneus reaching the posterior tubercles were seen (Fig. 2a, b).

Group F/sustentacular lamellae

From the sustentaculum tali, thick trabeculae converged downwards to join the thickened compacta of the medial wall of calcaneus. These were crossed, at right angles, by lamellae which were directed horizontally (Fig. 1a).

In the medial part of body, below the posterior part of the sustentaculum, there were wavy horizontal plates extending from the cortex joining the sagittally oriented plates of the Group B lamellae (Fig. 1b).

After examining sections in sagittal, coronal and horizontal planes, reinforced by the findings of gross dissection, a wedge-shaped area of sparse trabeculae was observed in the antero-inferior part of the calcaneus. This area had a medial and a lateral wall, antero-superior and postero-superior walls and a base was observed in all the bones. Its postero-superior wall was formed by Group B lamellae and antero-superior wall was formed by the Group C lamellae. Its edge was directed superiorly which extended from side to side and coincided with the cortical thickening anterior to the posterior talar facet. A vertical column of trabeculae extended from the thickened edge to the anterior tubercle inferiorly. This divided the triangle into a smaller anterior and a larger posterior part (Fig. 2a, b). The small anterior part tended to obliterate in lateral sagittal sections because of the presence of vertical components of Group C lamellae present there (Fig. 5a, b). Within the triangle, there were very fine and sparse bony strands filling up the space.

Discussion

The cortex of the calcaneus was thick along the medial wall, especially postero-inferior to the sustentaculum tali, suggesting that the load received by the sustentaculum tali is transferred through the compacta, onto the medial tubercle of the calcaneus. Albright et al. [1] suggest that the cortical bone not only interacts with the trabeculae to transmit mechanical forces, but can also carry much of the load itself. While describing the transmission of various forces through the cortex, they have stated that thicker areas of

compacta are for greater stress and thickness closely parallels the functional needs at each level. The thin compact bone especially along the antero-inferior part of the lateral wall explains the characteristic lateral wall blowout in the fractures of calcaneus.

The distinct transverse thickening of the compact bone, which was observed just in front of the anterior edge of posterior talar facet, was in the roof of triangular rarified area. The angle of Gissane is often described as a radiological entity, represented by two strong cortical struts that extend laterally and form an obtuse angle. The first strut extends along the lateral border of the posterior facet, and the second extends anteriorly to the beak of the calcaneus [16, 25]. We suggest that the angle of Gissane is not just an intersection of lines, but an intersection of two planes. The thickening of the compact bone which has been demonstrated is along the intersection of these two planes. It extends transversely (mediolateral) between posterior talar facet and the anterior part of the superior surface of the calcaneus. When the talus is axially loaded, the compressive force is passed onto the calcaneus in two different directions: postero-inferiorly from the posterior talar facet and antero-inferiorly through the middle and anterior talar facets. As a result of this, a net tensile effect is generated along the angle of Gissane. Similar tensile forces are generated, along the same area, when the ground reaction forces act in the opposite direction. The strong cortical thickening along this angle appears to be reinforcement for resisting these tensile forces (Fig. 7). Incidentally, this thickening also supports the lateral process of talus astride it. Available literature does not focus on this functionally, hence clinically, very important aspect of the calcaneus.

Calcaneal fractures typically occur because of axial loading as a result of high-energy trauma, usually due to a fall from a height, with the patient's weight being concentrated on the heels on landing [7, 25]. It is expected that, in such situations, larger amounts of ground reaction forces (impact forces) are generated and transmitted in opposite direction, so that the net tensile effect which is generated at the Gissane angle exceeds beyond normal limits. This may lead to creation of a fracture line either just anterior or posterior to the cortical thickening at the angle of Gissane. It is known that the primary fracture line that divides the calcaneus into anterior and posterior portions starts laterally from the angle of Gissane and runs medially [5, 6]. However, as proposed earlier, our view is contrary to the general contention that the lateral process of the talus that is astride the Gissane angle acts as an axe and results in production of this primary fracture line [20, 24].

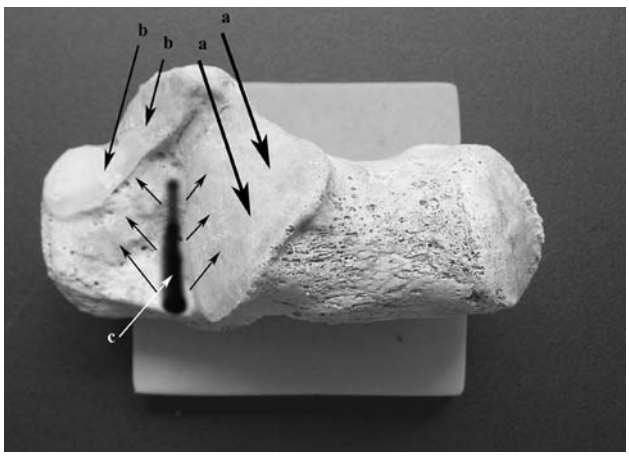

Fig. 7 Superior surface of the calcaneus showing compressive forces acting on the posterior talar facet (directed postero-inferiorly *a*,*a*) and on the anterior and intermediate talar facet (directed antero-inferiorly *b*,*b*) resulting in a net tensile effect created along area *c*

There has been a general consensus that the tensile forces act on inferior aspect of the calcaneus. The thickening that has been observed in the present study, in the compact bone of the inferior surface deep to the long plantar ligament, seems to be due to the condensation of tensile lamellae. Tensile forces are maximal along the inferior surface of the calcaneus due to the pull by tendocalcaneus and plantar ligaments and fascia. This thickening appears to resist the tensile forces along this surface. Similar view has been expressed by Williams et al. [31].

Trabecular pattern of calcaneus

The trabecular patterns are clearly a pragmatic solution to a number of varied and changing problems throughout the foot structure.

Wolff [32] had likened the internal structure of the calcaneus in sagittal section to the upper end of the femur, where the lamellae cross at right angles. Closely packed parallel bony tubes were observed extending from the upper part of posterior talar facet posteriorly to an area above the attachment of tendocalcaneus (Group A). The presence of these lamellae is well illustrated in the works of von Meyer [30]. But Thompson's illustration (as depicted by Bacon et al. [3]) does not show these lamellae. Bacon et al. [3] and Gefen et al. [10] have identified this group and attributed it to the anticlockwise pull exerted by the tendocalcaneus. According to us, these trabeculae form a rigid short arm of the lever during the movements of the ankle joint; while the fulcrum is located at the ankle joint. These trabeculae provide optimal length to the calcaneus (i.e. to the short arm of the lever) for efficient action of the tendocalcaneus. These trabeculae act as a strut, which prevents the buckling effect produced by the powerful pull exerted by the strong tendocalcaneus, during plantar flexion at the ankle joint. It does not appear to be directly related to the pull of tendocalcaneus, as its site of attachment is inferior to this group of trabeculae.

This group has remained unnoticed by other workers who have tended to merge it with Group B lamellae [26,

29]. According to us, these two groups of lamellae (Groups A and B) have different orientation, structure and function.

The Group B which was directed posterior-inferiorly from posterior talar facet is suited to transmit the compressive forces brought from the talus to the posterior talar facet of calcaneus onto the heel. The sagittal plates present here can conveniently receive the compressive forces from the talus via the vertical plates in the body of the talus as described by Athavale et al. [2]. Although this group of lamellae has been documented and illustrated by various workers, its precise structure and orientation have not been reported earlier [3, 14, 30, 32].

Conflicting views have been proposed for the Group C lamellae. The available descriptions do not account for the transmission of forces to the cuboidal facet. Wood Jones suggested that this group arises from the posterior talar facet; however, Takechi et al. and Kapandji et al. report it to be arising from Gissane angle [14, 29, 33]. No study has elaborated on the origin, precise nature and orientation of these lamellae. As already described, vertical sagittal plates deep to the posterior talar facet along their posterior ends continue as Group B lamellae. We have observed and demonstrated that the inferior ends of the same plates proceed in forward direction, in their course impinge onto the thick bony strut at angle of Gissane, and the lamellae further radiate towards the cuboidal facet. This observation provides a logical explanation that a part of force received at the posterior talar facet passes onto the cuboid through this group of lamellae. An important finding in the present study was the stacked plate like arrangement of these lamellae, which when traced distally, inclined downwards and laterally. Such a contour of the plates conforms to the anatomical position of the cuboid and hence convenient for transmitting the compressive forces to the anterior limb of the lateral longitudinal arch of the foot.

There is a general consensus regarding the Group D lamellae. These trabeculae resist traction forces and can be explained on the basis of traction exerted by tendocalcaneus, plantar aponeurosis, long and short plantar ligaments and intrinsic muscles of the sole [3, 14, 24, 26].

The Group E lamellae in the form of stacked plates have received little attention. This arrangement resists the pull by tendocalcaneus as is also deduced by Kachlik et al. [13].

The presence of neutral triangle as described by Wood Jones and Harty has been substantiated time and again [12, 33]. Sabry et al. [24] described the 3D extent of this triangle and the presence of a partial vertical septum dividing this triangle. Our findings conform to the findings of Sabry et al. with following additional points: This rarified zone was observed in all the bones studied. The thickened compacta which is present at the angle of Gissane which forms the roof/edge seems to reinforce the roof of the weak wedge-shaped region situated inferiorly. The vertical column that divides the zone into anterior and posterior parts is complete and extends from the roof to the floor that seems to function as a support beam. The amount of trabeculae filling this space varies, so this part of the calcaneus can be utilized for assessment of osteoporosis.

Fernandez et al. [9] in their densitometric analysis of the trabecular bone of the calcaneus have identified the anterosuperior region and the posterior regions having the highest bone mineral densities. These regions correspond with the proximal part of Group B lamellae and Group C, E and F lamellae where we have observed the presence of lamellae in the form of plates and hence dense. The least bone mineral density area corresponds well with the position of neutral zone.

Classification of fractures of calcaneus has been a matter of intense investigation [25]. The fracture lines and fragments that are produced in calcaneal fractures should have a correlation with the internal architecture and major lamellar groups. The vulnerable cleavage areas run in between the major lamellar groups or within a lamellar group along the weaker interconnections between the lamellae (Figs. 8, 9). Primary fracture line shears the calcaneus into medial and lateral portions [5, 6, 20]. This can be explained on the basis of preferential orientation of the lamellae in sagittal plane within the calcaneus; the shear forces may disrupt the horizontal bridges between the plates and produce a plane of cleavage running antero-posteriorly. The anterior extension of this line runs between the Group C and the sustentacular group splitting the cuboidal facet. As the sustentacular group impinges onto the medial wall of calcaneus, it stays together with the medial fragment in a sagittal split of the calcaneus. An anterolateral fragment is separated out as a result of another primary fracture line along the angle of Gissane [29, 33]. This fragment bears the Group C lamellae. Miric et al. [20] reported the occurrence of anterolateral fragment in 93% cases studied. The superomedial and superolateral fragments as described by Sanders are a result of cleavage between Group A and B lamellae [25]. The primary fracture line as described by Wuelker [34] coincides with lower margin of Group B lamellae, where they form the posterior boundary of neutral triangle. In joint-depression fracture described by Essex-Lopresti [8], a transverse fracture in the coronal plane of the calcaneus develops between the posterior facet and the insertion of the tendocalcaneus. The location of the transverse fracture forces the posterior facet inferiorly. This fracture line coincides with the posterior edges of the sagittal plates deep to the posterior articular facet where they split and become continuous with rods of Group B lamellae.

It is now increasingly being acknowledged that the structural changes of trabecular bone are more important in predicting osteoporotic fractures than the measurements of bone mineral density alone. In age-related osteoporosis, the bone undergoes adaptive remodeling. This process preferentially

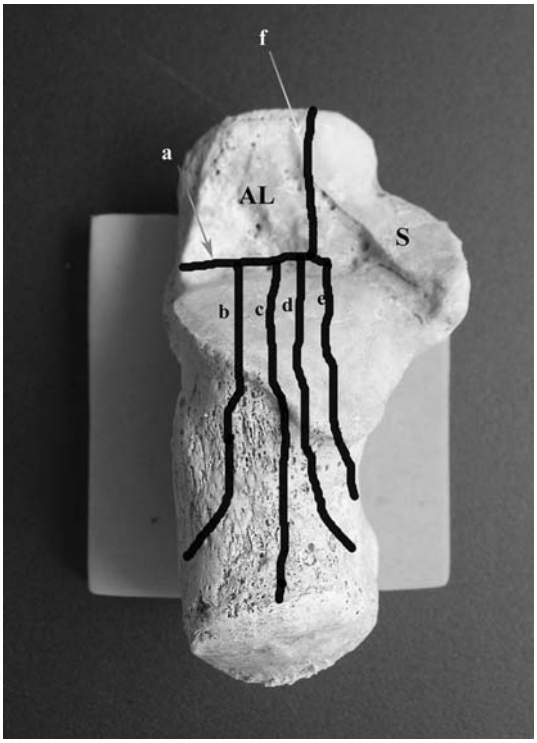

Fig. 8 Showing superior surface of the left calcaneus showing surface projection of potential vulnerable areas in the calcaneus. A coronal weak zone along the anterior border of posterior talar facet either anterior or posterior to the thickened compact bone along the Gissane angle; *b*, *c*, *d*, *e* represent sagittal weak zones along the horizontal cross bridges between the sagittal plates deep to posterior talar facet. *f* represents a zone between the 'Group C' and 'Group F' (sustentacular) lamellae. *AL* anterolateral fragment, *S* sustentacular fragment

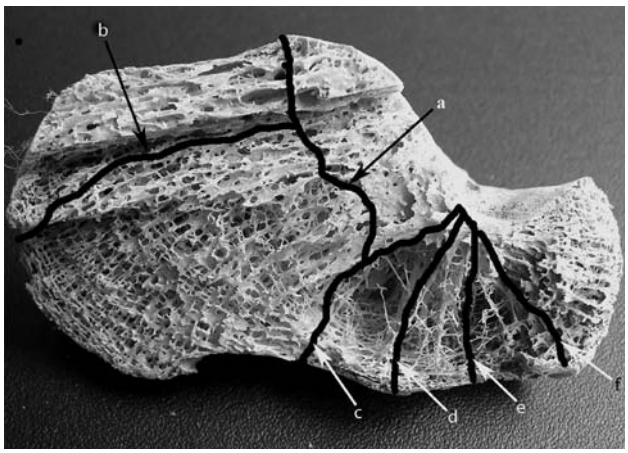

Fig. 9 Showing gross dissection of right calcaneus showing vulnerable cleavage in the calcaneus. *a* Along the posterior margins of the sagittal plates of 'Group B' lamellae where they split into thin plates and then rods and curve downwards. *b* Between the A and B groups of lamellae; *c*, *d*, *e*, *f* Along the boundaries and subdivisions of the neutral zone

preserves or adds bone mass to the areas subjected to high load and resorbs unloaded or redundant areas [19]. In such cases, thinner trabeculae and the cross bridges between the main lamellar patterns are lost. This results in further weakening of the existing weaker zones of the bone (intra- or inter-group weak zones) and hence predisposes to fractures.

Calcaneus has also been frequently utilized for investigation of trabecular bone using various modalities because of abundance of trabecular bone present here and its easy accessibility. Here, trabecular bone has been a preferential site for densitometric analysis and assessment of trabecular structure for predicting osteoporotic changes [9, 17, 27]. The findings may be gainfully utilized in selection of appropriate sites for densitometric, structural and textural studies of trabecular bone of the calcaneus.

Conclusions

Internal architecture of calcaneus has been described as several groups of lamellae. The present study was focused on elaborate description of the precise nature and orientation of the individual groups. Weaker zones depending on the internal architecture of the bone have been identified. In coronal plane, these zones lie just anterior or posterior to the thick compacta at the angle of Gissane and at the posterior ends of the sagittal plates deep to the posterior talar facet. In sagittal plane, the weaker zones lie along the interconnections between the Group B lamellae and further anteriorly between Group C and sustentacular group of lamellae. In horizontal plane, a weak zone is present between Group A and Group B lamellae. Weaker zones also exist along the boundaries of the neutral triangle and its subdivisions. The fracture lines of the calcaneus may run through a single or multiple weak zones.

As is evident from the above discussion, the fracture lines in the calcaneus not only correlate well with the weaker zones identified in the study but also provide anatomical basis for their occurrence. This study underscores the major influence of the internal architecture of the calcaneus in predicting the fracture lines.

Treatment of calcaneal fracture depends on its classification, but the classification of the fractures has been a matter of debate since long. The available classifications have not taken into account the internal structure of this bone. Findings of this study will help in proper classification of these fractures and hence in the treatment. Knowledge of these weak zones will aid the orthopedic surgeons to improve the techniques of internal fixation.

References

1. Albright JA (1987) Bone physical properties. In: Albright JA, Brand RA (eds) The scientific basis of orthopaedics, 2nd edn. Appleton and Lange, California, pp 213–239

2. Athavale SA, Joshi SD, Joshi SS (2008) Internal architecture of the talus. Foot Ankle Int 29:82–86
3. Bacon GE, Bacon PJ, Griffiths RK (1984) A neutron diffraction study of the bones of the foot. J Anat 139:265–273
4. Barei DP, Bellabarba C, Sangeorzan BJ et al (2002) Fractures of the calcaneus. Orthop Clin North Am 33:263–268
5. Carr JB (1993) Mechanism and pathoanatomy of the intraarticular calcaneal fracture. Clin Orthop Relat Res 290:36–40
6. Carr JB, Hamilton JJ, Bear LS (1989) Experimental intra-articular calcaneal fractures: anatomical basis for a new classification. Foot Ankle 10:81–87
7. Daftary A, Haims AH, Baumgaertner MR (2005) Fractures of the calcaneus: a review with emphasis on CT. RadioGraphics 25:1215–1226
8. Essex-Lopresti P (1952) The mechanism, reduction technique, and results in fractures of the os calcis. Br J Surg 39:395–419
9. Fernandez FJ, Morante MP, Rodriguez RT et al (1996) Densitometric analysis of the human calcaneus. J Anat 189:205–209
10. Gefen A, Seliktarb R (2004) Comparison of the trabecular architecture and the isostatic stress flow in the human calcaneus. Med Eng Phys 26:119–129
11. Giddings VL, Beaupré GS, Whalen RT et al (2000) Calcaneal loading during walking and running. Med Sci Sports Exerc 32:627–634
12. Harty M (1973) Anatomic considerations in injuries of the calcaneus. Orthop Clin North Am 4:179–183
13. Kachlik D, Baca V, Cepelik M et al (2008) Clinical anatomy of the calcaneal tuber. Ann Anat 190(3):284–291
14. Kapandji JA (1987) Physiology of the joints, 5th edn. Churchill Livingstone, Edinburgh
15. Kersting UG, Bruggemann GP (1999) Adaptation of the human calcaneus to variations of impact forces during running. Clin Biomech 14:494–503
16. Knight JR, Gross EA, Bradley GH et al (2006) Boehler's angle and the critical angle of Gissane are of limited use in diagnosing calcaneus fractures in the ED. Am J Emerg Med 24:423–427
17. Lin JC, Amling M, Newitt DC et al (1998) Heterogeneity of trabecular bone structure in the calcaneus using magnetic resonance imaging. Osteoporos Int 8:16–24
18. Lowery RBW, Calhoun JH (1996) Fractures of the calcaneus. 1. Anatomy, injury mechanism, and classification. Foot Ankle Int 17:230–235
19. Mc Donnell P, Mc Hugh PE, O' Mahoney D (2007) Vertebral osteoporosis and trabecular bone quality. Ann Biomed Eng. doi:10.1007/s10439-006-9239-9
20. Miric A, Patterson BM (1998) Pathoanatomy of intra-articular fractures of the calcaneus. J Bone Joint Surg 80:207–212
21. Paley D, Halls H (1993) Intra-articular fractures of the calcaneus—a critical analysis of results and prognostic factors. J Bone Joint Surg Am 75:342–354
22. Plaue R, Oellers B, Salditt G (1977) Experiment studies on fractures of the human calcaneus under vertical pressure. Arch Orthop Unfallchir 88:19–25
23. Rammelt S, Zwipp H (2004) Calcaneus fractures: facts, controversies and recent developments. Injury 35:443–461
24. Sabry FF, Ebraheim NA, Mehalik JN et al (2000) Internal architecture of the calcaneus: implications for calcaneus fractures. Foot Ankle Int 21:114–118
25. Sanders R (2000) Current concepts review: displaced intra-articular fractures of the calcaneus. J Bone Joint Surg Am 82:225–250
26. Sinha DN (1985) Cancellous structure of tarsal bones. J Anat 140:111–117
27. Sone T, Imai AY, Tomomitsu AT et al (1998) Calcaneus as a site for the assessment of bone mass. Bone 22:155S–157S
28. Steindler A (1914) On the architecture of the tarsus. J Bone Joint Surg Am 2:275–302
29. Takechi H, Shiro I, Toshiya T, Hiroshi N (1982) Trabecular architecture of the ankle joint. Anat Clin 4:227–233
30. von Meyer GH (1867) Die architektur der spongiosa [German]. Arch Anat Physiol Wiss Med 34:615–628
31. Williams PL, Bannister LH, Berry MM et al (1995) Gray's anatomy, 38th edn. Churchill Livingstone, London
32. Wolff J (1892) Das Gesetz der Transformation der Knochen. Verlag von August Hirschwald, Berlin
33. Wood Jones F (1953) Buchanan's manual of anatomy, 8th edn. Bailliere, Tindall and Cox, London
34. Wuelker N, Zwipp H (1996) Fracture anatomy of the calcaneus with axial loading. Cadaver experiments. Foot Ankle Surg 2:155–162
35. Yoganandan N, Pintar FA, Seipel R (2000) Experimental production of extra- and intra-articular fractures of the os calcis. J Biomech 33:745–749
36. Zwipp H, Tscherne H, Thermann H et al (1993) Osteosynthesis of displaced intraarticular fractures of the calcaneus—results in 123 cases. Clin Orthop Relat Res 290:76–86